Available online at www.sciencedirect.com
SCIENCE DIRECT®
Catalysis Today 89 (2004) 205–211
CATALYSIS TODAY
www.elsevier.com/locate/cattod

Plasma-chemical preparation of nanostructured catalysts for low-temperature steam conversion of carbon monoxide: thermodynamic and model studies

Gheorghy P. Vissokov*

Institute of Electronics, Bulgarian Academy of Sciences, 72 Tsarigradsko Chaussee Bulvd., 1784 Sofia, Bulgaria

Abstract

A universal program has been used and, for a first time, the equilibrium parameters of the multicomponent heterogeneous system Cu–Zn–Al–O in two variants of the initial ingredient composition at a pressure of 0.1 MPa within the temperature range from 1000 to 3700 K have been defined, as dependencies of the concentration of the corresponding compound in gas and condensed phase at an equilibrium composition of the system on the temperature have been build.

Devising 2D models that describe the motion, heating, melting and vaporization (thermal destruction) of micron-size particles in an axisymmetric cylindrical plasma-chemical reactor (PCR) (with "cold" ($T_W = 500$ K) (CW) or "warm" ($T_W = 1500$ K) (WW) walls), is invaluable in obtaining sufficiently accurate data enabling one to determine the optimal plasma-chemical process parameters: PCR size, time of residence of the particles in it, as well as the particle diameter changes along the length of the PCR; trajectory of the particles in the PCR, etc.

Based on the model calculations, we designed and built a plasma-chemical installation and used it to study the mechanisms of preparation of catalysts (and regeneration of spent deactivated catalysts) for low-temperature steam conversion of carbon monoxide.

Keywords: Plasma-chemical preparation; Nanostructured catalysts; Low-temperature steam conversion of carbon monoxide; Thermodynamic and model studies

1. Introduction

The three main trends in the plasma-chemical synthesis of catalysts are: (1) plasma-chemical preparation and activation of catalysts in the condensed phase; (2) plasma-assisted deposition of catalytically active compounds and composites on various carriers and (3) plasma enhanced preparation or plasma modification of catalysts.

The first investigations on plasma-chemical preparation of nanostructured catalysts for low-temperature steam conversion of carbon monoxide (LTSCCO) were found in the periodical and licensed literature [1–8].

2. Methods

2.1. High-temperature thermodynamics of the Cu–Zn–Al–O system

The literature review made shows that there are some data on the plasma-chemical synthesis (PCS) of catalysts for LTSCCO in the specialized literature [1–8], but there are missing reports on plasma-chemical regeneration of already processed catalysts. Data are missing on the equilibrium parameters of the multicomponent heterogeneous Cu–Zn–Al–O system that is used as a base for some conventional catalysts for LTSCCO. For that purpose an universal program for determination of multicomponent heterogeneous systems equilibrium parameters has been used [5], at a pressure of 0.1 MPa for the temperature range of 1000–3700 K (with a step of 300 K).

* Fax: +359-2-9753-201.
E-mail address: marinela_panayotova@hotmail.com (G.P. Vissokov).

0920-5861/$ – see front matter © 2003 Elsevier B.V. All rights reserved.
doi:10.1016/j.cattod.2003.11.028

2.2. Motion and vaporization of micron-size particles in an axisymmetric cylindrical PCR

The theoretical and experimental studies of the processes mentioned are hampered by the short duration and the non-steady state and spatially non-uniform character of the accompanying phenomena, as well as by the multiple determining factors and their complex interdependence.

The equations we used to model the hydrodynamic and heat exchange-processes in a cylindrical axisymmetric PCR were presented in [9–12].

3. Results and discussion

We calculated the equilibrium content of the Cu–Zn–Al–O system within the 1000–3700 K interval (step of 300 K) for a pressure of 0.1 MPa and for the initial ingredient content (mol/kg)—first variant: Cu, 3.7709 mol/kg (23.96 mass%); Zn, 5.5313 mol/kg (36.16 mass%); Al, 4.9011 mol/kg (13.22 mass%); and O, 16.654 mol/kg (26.65 mass%) (Fig. 1) and second variant: Cu, 1.1097 mol/kg (7.05 mass%); Zn, 1.6278 mol/kg (10.64 mass%); Al, 1.4424 mol/kg (3.89 mass%); and O, 49.011 mol/kg (78.42 mass%) (Fig. 2).

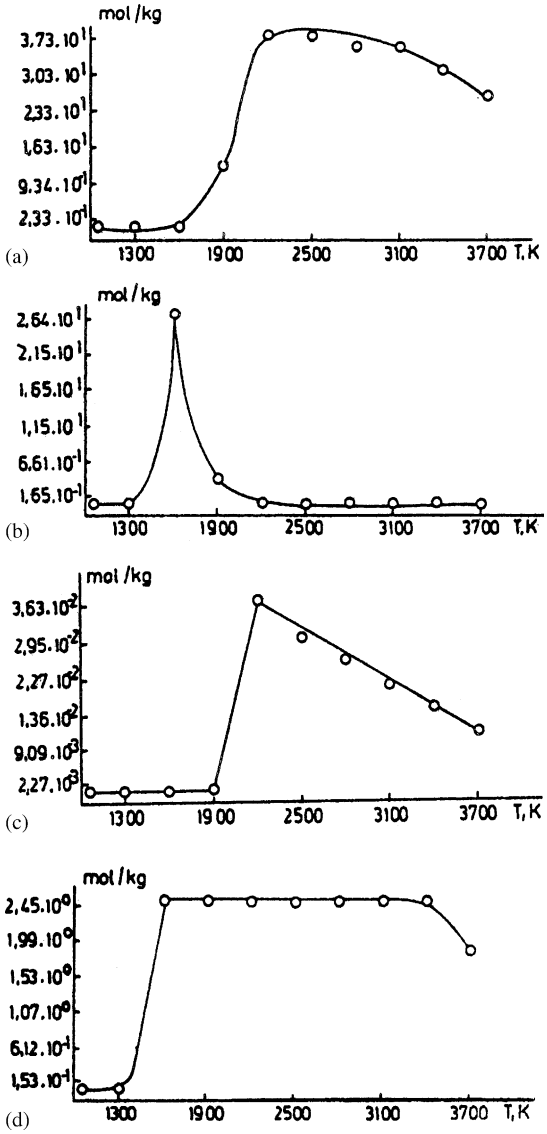

Fig. 1. Concentration (mol/kg) of some compounds in gas or condensed (K*) phase at equilibrium composition of the Cu–Zn–Al–O system (first variant) depending on the temperature, T (K): (a) CuO concentration at equilibrium composition of the Cu–Zn–Al–O system depending on the temperature; (b) concentration of K* CuO (mol/kg) at equilibrium composition of the Cu–Zn–Al–O system depending on the temperature; (c) ZnO concentration (mol/kg) at equilibrium composition of the Cu–Zn–Al–O system depending on the temperature; (d) concentration of K* Al_2O_3 at equilibrium composition of the Cu–Zn–Al–O system depending on the temperature.

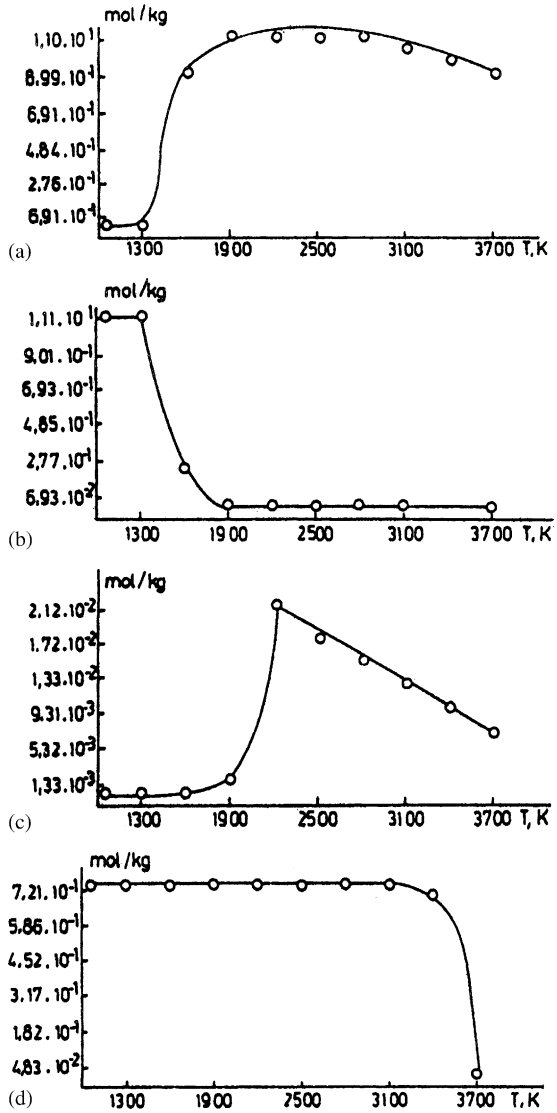

Fig. 2. Concentration (mol/kg) of some compounds in gas or condensed (K*) phase at equilibrium composition of the Cu–Zn–Al–O system (second variant) depending on the temperature, T (K): (a) CuO concentration at equilibrium composition of the Cu–Zn–Al–O system depending on the temperature; (b) concentration of K* CuO (mol/kg) at equilibrium composition of the Cu–Zn–Al–O system depending on the temperature; (c) ZnO concentration (mol/kg) at equilibrium composition of the Cu–Zn–Al–O system depending on the temperature; (d) concentration of K* Al_2O_3 at equilibrium composition of the Cu–Zn–Al–O system depending on the temperature.

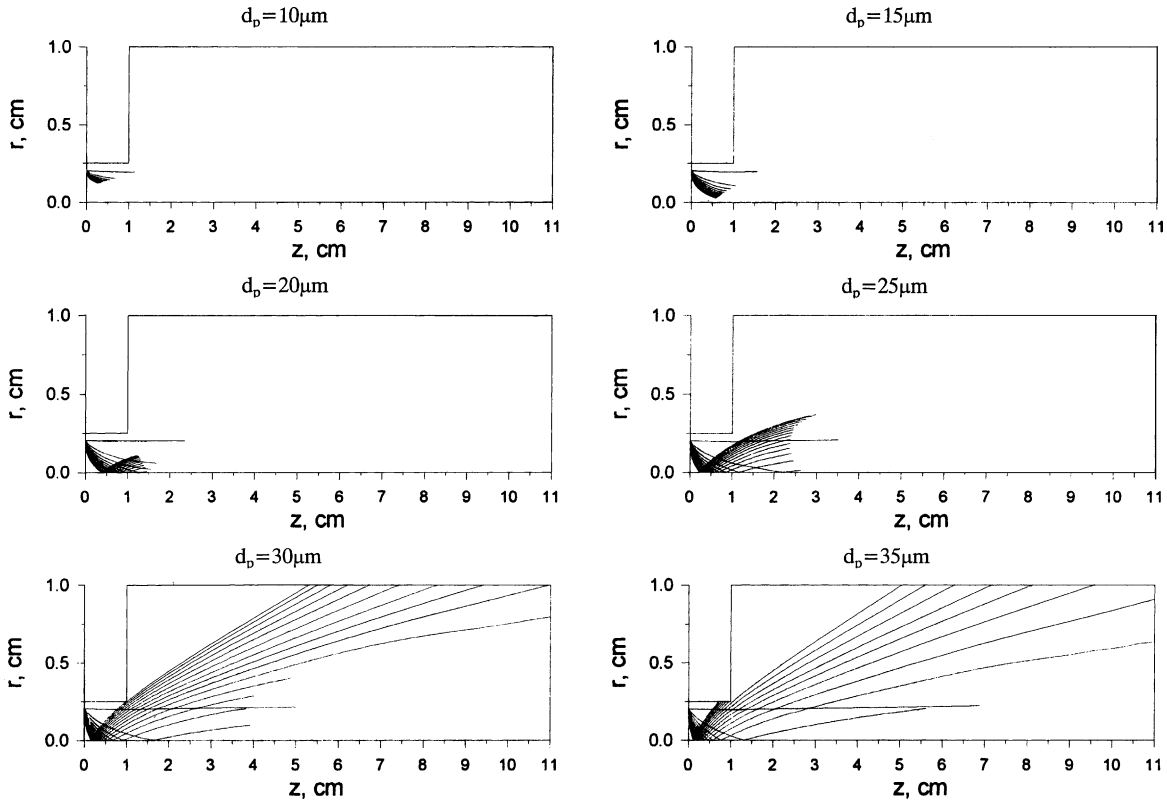

Fig. 3. Trajectories of motion of Al particles with equivalent diameters of 10, 15, 20, 25, 30, 35 μm in a CW PCR (breaking of trajectory indicates vaporization of the particle).

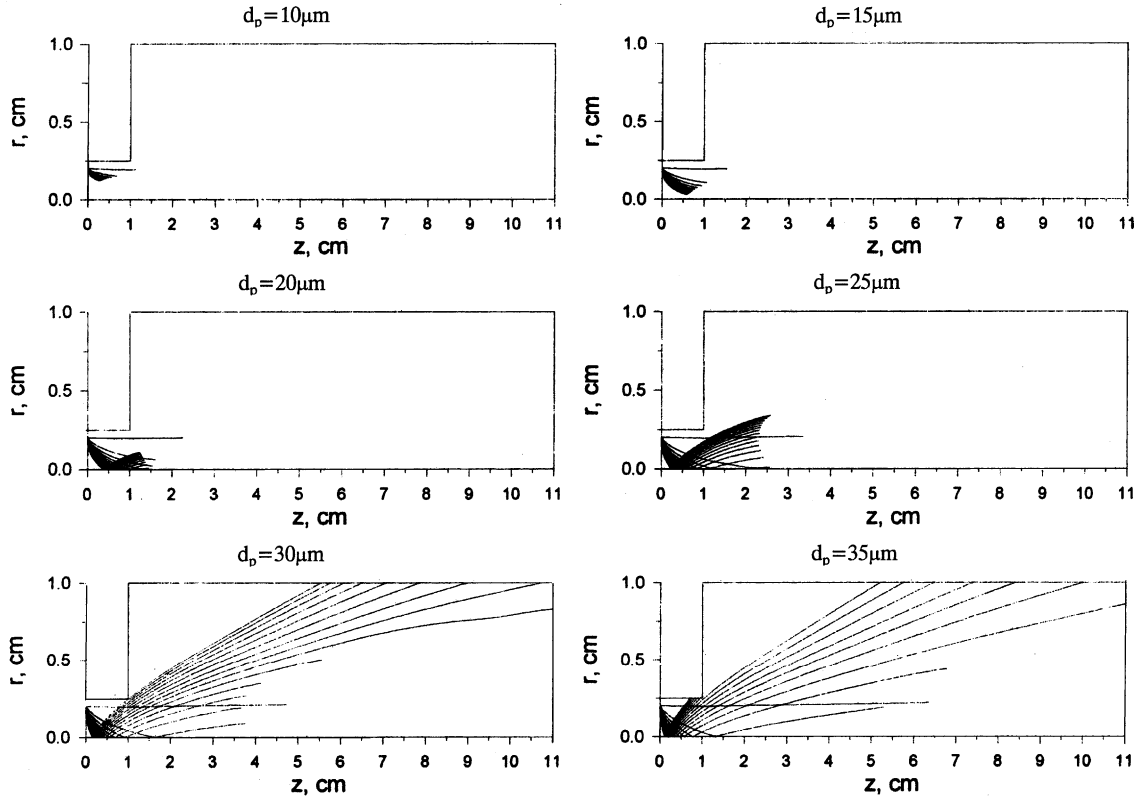

Fig. 4. Trajectories of motion of Al particles with equivalent diameters of 10, 15, 20, 25, 30, 35 μm in a WW PCR (breaking of trajectory indicates vaporization of the particle).

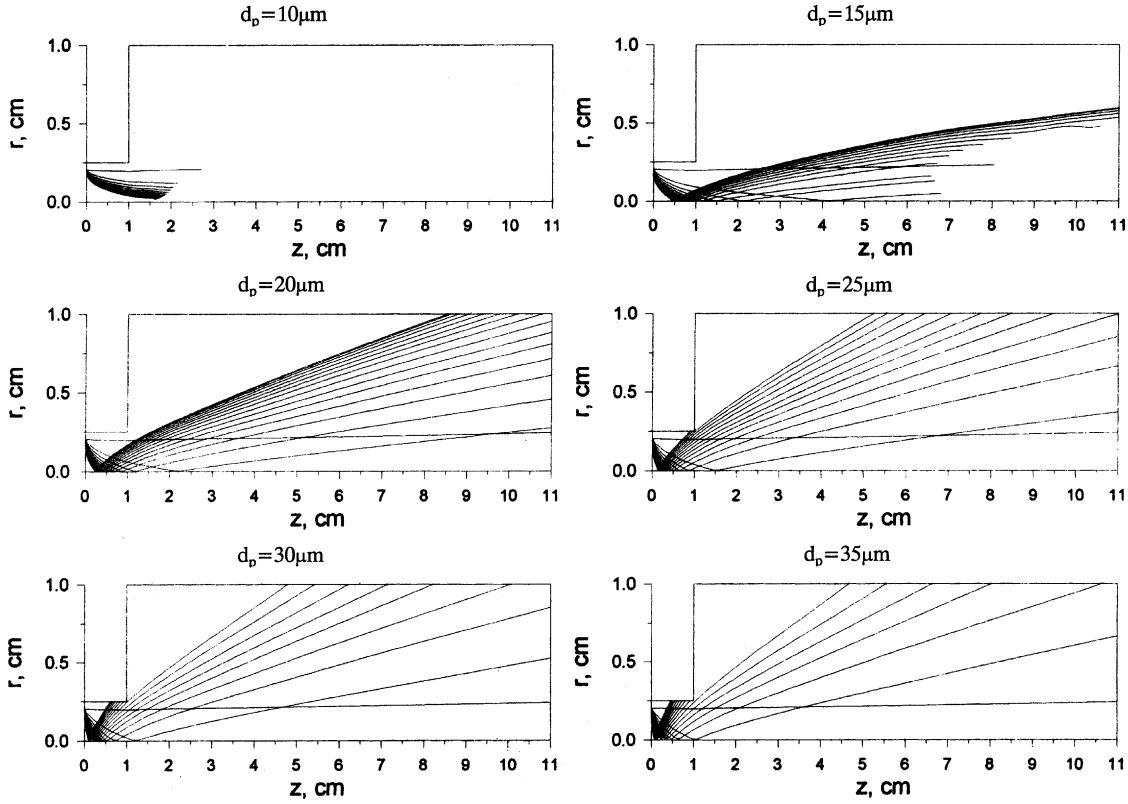

Fig. 5. Trajectories of motion of Al_2O_3 particles with equivalent diameters of 10, 15, 20, 25, 30 and 35 μm in a CW PCR (breaking of trajectory indicates vaporization of the particle).

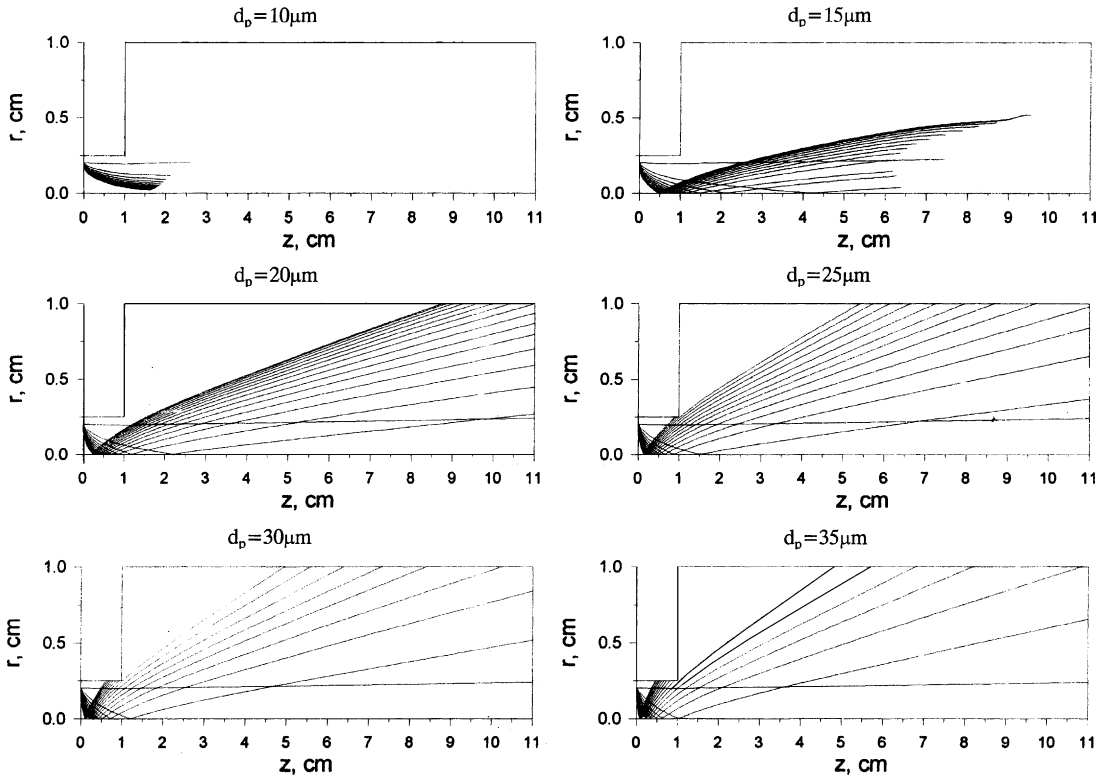

Fig. 6. Trajectories of motion of Al_2O_3 particles with equivalent diameters of 10, 15, 20, 25, 30 and 35 μm in a WW PCR (breaking of trajectory indicates vaporization of the particle).

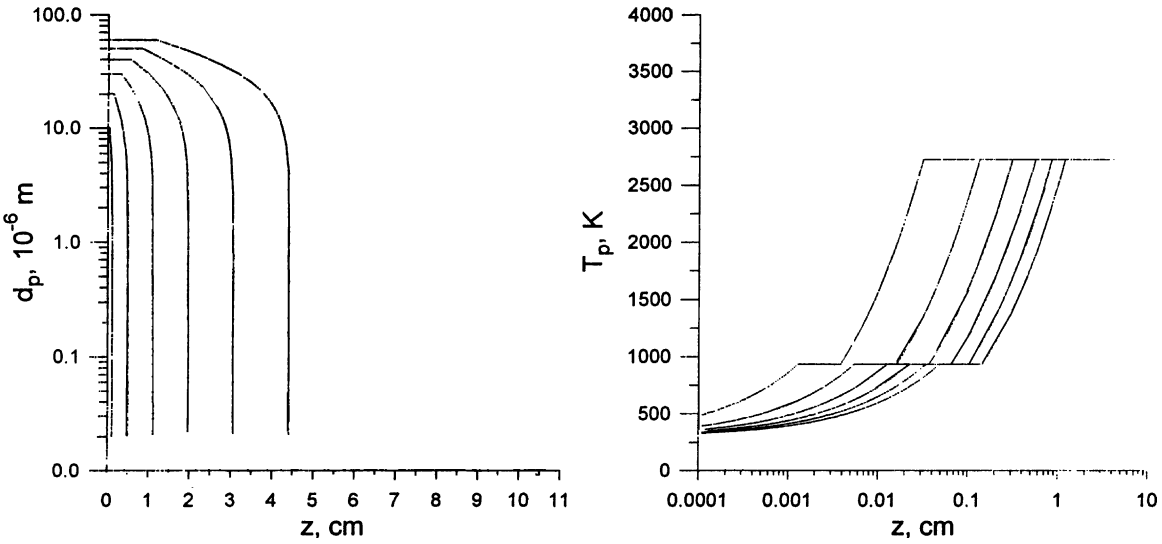

Fig. 7. The particle diameter (d_p, m) (from left to right 10, 15, 20, 25, 30 and 35 μm) and temperature (T_p, K) of Al particles changes along the length (z, cm) of the CW PCR.

The analysis of results of the thermodynamics calculations for both Cu–Zn–Al–O system composition variants witnesses that within the temperature range 1000–3700 K, at high temperatures (above 2000 K), the system contains in gas phase mainly CuO and ZnO.

In the condensed phase, was the main component ZnO in the equilibrium composition at temperature up to 1900 K and Al_2O_3—at temperature up to 3500 K. Thermodynamics calculation were also done for temperatures above 6000 K, at which all components are in gas phase as radicals, molecules of the corresponding elements, and ions and electrons. Due to the fact that our practical interest is directed to the products in condensed phase, those results are not represented in the present article. The thermodynamic probability for condensation of phases of the type $CuAl_2O_4$ and Cu_2O, which were observed in the analyzed phases by the X-ray structural analysis of plasma-chemically synthesized samples were not taken into account in the calculations.

The trajectories of motion of Al particles with equivalent diameters 10, 15, 20, 25, 30 and 35 μm are shown in Figs. 3 and 4 and of Al_2O_3 are shown in Figs. 5 and 6. As one can see, in a CW PCR (Fig. 3), the Al particles with equivalent diameter $d \leq 25$ μm are completely vaporized, the particles with $d = 30$ μm are vaporized up to 50%, while for $d = 35$ μm a substantial fraction of the particles leaves the PCR without being completely vaporized. In a WW PCR, the vaporization is improved insignificantly (Fig. 4). The following values were used in the calculations [5]: temperature of melting of Al, $T_m = 933$ K; temperature of Al

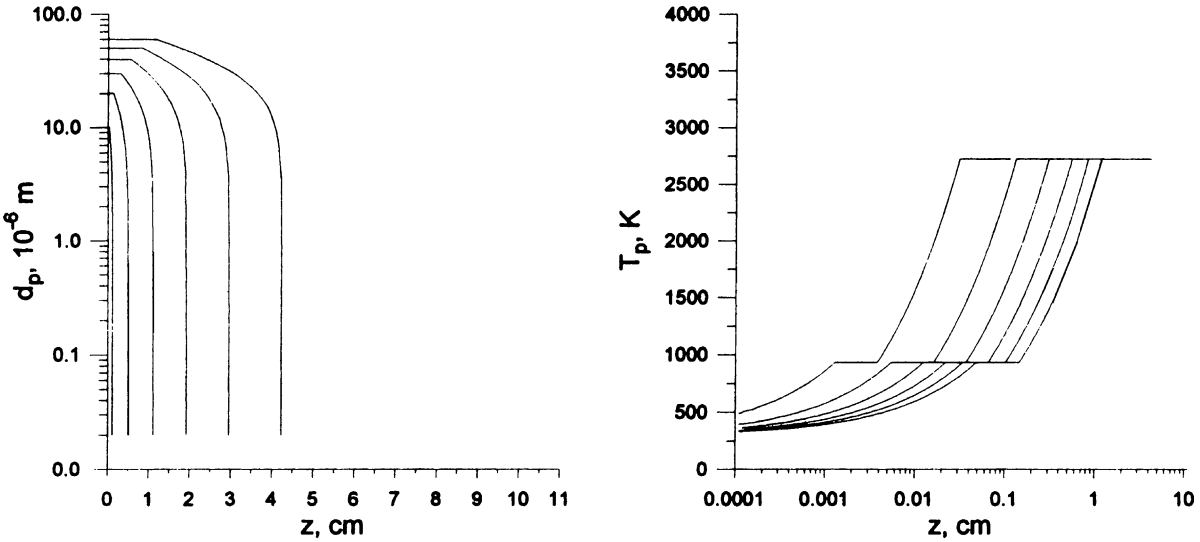

Fig. 8. The particle diameter (d_p, m) (from left to right 10, 15, 20, 25, 30 and 35 μm) and temperature (T_p, K) of Al particles changes along the length (z, cm) of the WW PCR.

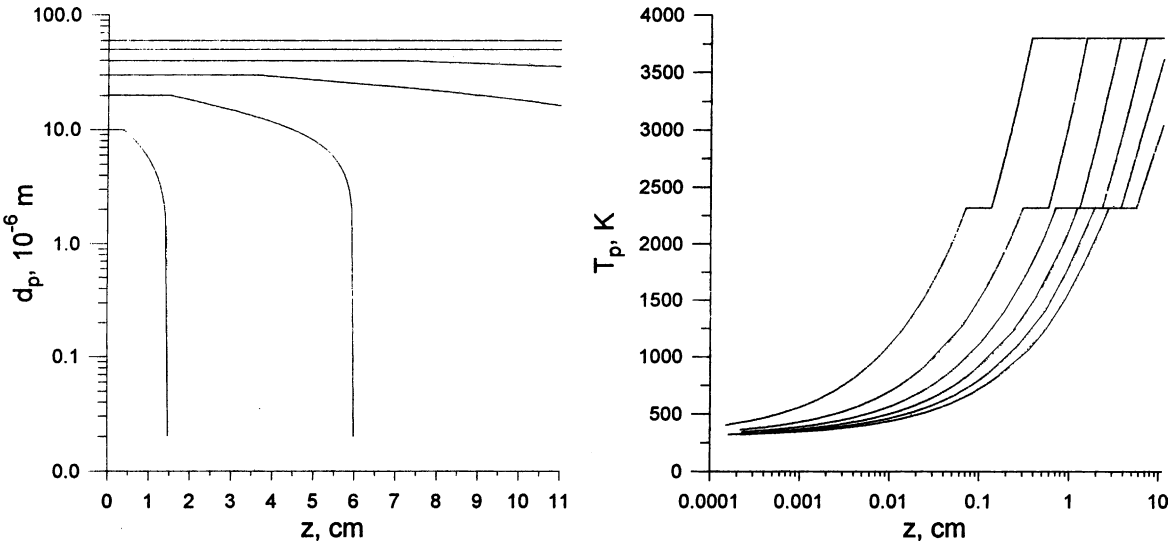

Fig. 9. The particle diameter (d_p, m) (from left to right 10, 15, 20, 25, 30 and 35 μm) and temperature (T_p, K) of Al_2O_3 particles changes along the length (z, cm) of the CW PCR.

boiling, $T_b = 2725$ K; $\rho_{293\,K} = 2.6989$ g/cm^3; $\rho_{1273\,K} = 2.289$ g/cm^3; $c_p^0 = 901.85$ J/kg K; $\Delta H^\circ_{melting} = 403.7$ kJ/kg; $\Delta H^\circ_{vap} = 11.19$ MJ/kg.

In a CW PCR (Fig. 5), the Al_2O_3 particles with equivalent diameter $d < 15$ μm are completely vaporized, the particles with $d = 15$ μm are vaporized up to 50%, while for $d = 20$ μm a substantial fraction of the particles leaves the PCR without being completely vaporized. In a WW PCR, the vaporization is improved insignificantly (Fig. 6).

In Figs. 7 and 8, we plotted the diameter and temperature variation of Al (Figs. 7 and 8) and Al_2O_3 (Figs. 9 and 10) micron-size particles along the length of a CW (Figs. 7 and 9) and WW (Figs. 8 and 10) PCR.

The particle radius (r_p, m) (from left to right 5, 10, 15, 20, 25 and 30 μm) and temperature (T_p, K) of CuO particles changes along the length (L_r, m) of the WW PCR we presented. As one can see, in a WW PCR (Fig. 11), the CuO particles with equivalent diameter $d = 20$ μm are completely vaporized, the particles with $d = 25$ μm are vaporized up to 50%, while for $d = 30$ μm a substantial fraction of the particles leaves the PCR without being completely vaporized.

Based on the results of the model calculations concerning the motion, heating, melting and vaporization of CuO and Al micron-size particles as presented above, we drew the conclusion that an axisymmetric CW or WW PCR (diameter $d_{PCR} = 2$ cm, length $z_{PCR} = 10$ cm, ingredients fed radially at 1 cm away from the plasmatron nozzle) can operate efficiently with particles with size of less than 20 μm with Ar used as a plasma-forming gas.

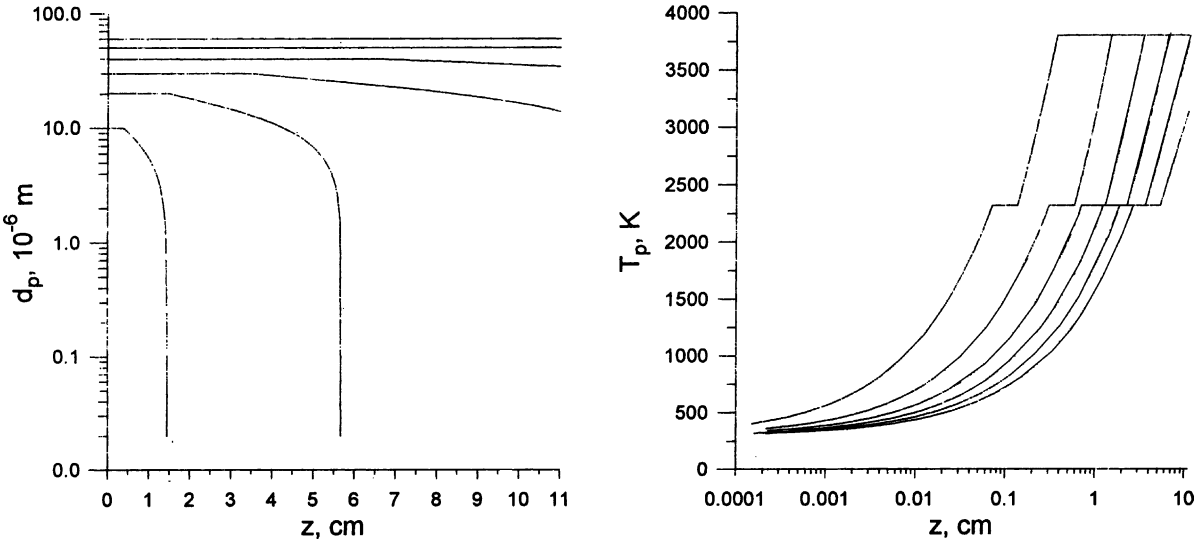

Fig. 10. The particle diameter (d_p, m) (from left to right 10, 15, 20, 25, 30 and 35 μm) and temperature (T_p, K) of Al_2O_3 particles changes along the length (z, cm) of the WW PCR.

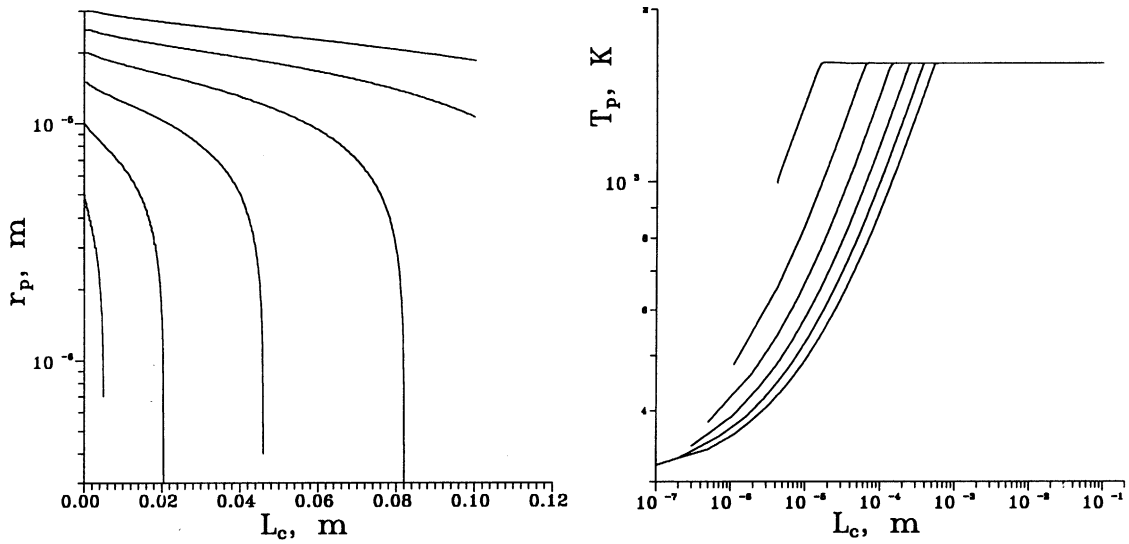

Fig. 11. The particle radius (r_p, m) (from left to right 5, 10, 15, 20, 25 and 30 μm) and temperature (T_p, K) of CuO particles changes along the length (L_r, m) of the WW PCR.

4. Conclusion

The technique we employed to calculate the free enthalpy of the multicomponent heterogeneous system Cu–Zn–Al–O enabled us to consider its state of equilibrium in the presence of powders, condensed-phase substances, and solid solutions. We were thus able to follow a large variety of equilibria, ranging from the condensed state to the plasma state of the substances present.

Devising 3D models that describe the motion, heating, melting and vaporization of micron-size particles in an axisymmetric cylindrical PCR with CW or WW, is invaluable in obtaining sufficiently accurate data enabling one to determine the optimal PCP parameters: PCR size, time of residence of the particles in it, as well as the particle diameter changes along the length of the PCR; trajectory of the particles in the PCR, etc.

Based on the model calculations, we designed and built a plasma-chemical installation and used it to study the mechanisms of preparation of catalysts (and regeneration of spent deactivated catalysts) for low-temperature steam conversion of carbon monoxide.

References

[1] A.M. Alexeev, E.V. Gorogankin, Izv. SSSR 238 (5) (1978) 1148.
[2] P.N. Tzibulev, V.D. Parhomenko, Proceedings of the Plasmachemistry'79, vol. 2, 1979, p. 60.
[3] J.E. Schenin, E.V. Gorogankin, Proceedings of the II Vsesoiuznogo soveschtanija po plasmochimitcheskoij tehnologii I apparaturostroeniu, vol. 1, 1977.
[4] J.E. Schenin, E.V. Gorogankin, Proceedings of the Plasmachemistry'79, vol. 2, 1979, p. 65.
[5] G.P. Vissokov, P.S. Pirgov, Nanodispersed Powders—Plasmachemical Synthesis and Properties, Sofia, Poliprint, 1998, p. 396.
[6] Iu.M. Schugov, Ph.D. Teses, 1971.
[7] A.S. Eliseeva, E.V. Gorogankin, Proceedings of the II Vsesoiuznogo soveschtanija po plasmochimitcheskoij tehnologii I apparaturostroeniu, vol. 1, 1977.
[8] A.S. Eliseeva, E.V. Gorogankin, Proceedings of the Plasmachemistry'79, vol. 1, 1979, p. 184.
[9] P.S. Pirgov, G.P. Vissokov, Chem. Ind. 69 (1) (1998) 9.
[10] G.P. Vissokov, P.S. Pirgov, in: A. Andreev, L. Petrov, Ch. Bonev, G. Kadinov, I. Mitov (Eds.), Proceedings of the Eighth International Symposium on Heterogeneous Catalysis, Varna, 1996, Acad. Publ. House, Sofia, 1996, p. 763.
[11] G.P. Vissokov, in: L. Petrov, Ch. Bonev, G. Kadinov, I. Mitov (Eds.), Proceedings of the Ninth International Symposium on Heterogeneous Catalysis, Varna, 2000, Acad. Publ. House, Sofia, 2000, p. 579.
[12] G.P. Vissokov, Catal. Today 72 (3–4) (2002) 197.